Vilnius
University
Press

Dynamics in diffusive Leslie–Gower prey–predator model with weak diffusion*

Xiao Wu[a] , **Mingkang Ni**[b,c,1]

[a]College of Science, Donghua University,
Shanghai 200000, China

[b]School of Mathematical Sciences,
East China Normal University,
Shanghai 200000, China

[c]Shanghai Key Laboratory of Pure Mathematics
and Mathematical Practice,
Shanghai 200000, China
xiaovikdo@163.com

Abstract. This paper is concerned with the diffusive Leslie–Gower prey–predator model with weak diffusion. Assuming that the diffusion rates of prey and predator are sufficiently small and the natural growth rate of prey is much greater than that of predators, the diffusive Leslie–Gower prey–predator model is a singularly perturbed problem. Using travelling wave transformation, we firstly transform our problem into a multiscale slow-fast system with two small parameters. We prove the existence of heteroclinic orbit, canard explosion phenomenon and relaxation oscillation cycle for the slow-fast system by applying the geometric singular perturbation theory. Thus, we get the existence of travelling waves and periodic solutions of the original reaction–diffusion model. Furthermore, we also give some numerical examples to illustrate our theoretical results.

Keywords: Leslie–Gower prey–predator model, geometric singular perturbation theory, relaxation oscillation, canard explosion phenomenon, heteroclinic orbit.

1 Introduction

The abundant dynamical feature of interacting species is a hot issue in the research of ecological system. Based on laboratory experiments and observations, researchers have proposed many realistic biological models such as prey–predator model. Among these models, a typical one is the Leslie–Gower prey–predator model, which is firstly proposed in [19]. In the Leslie–Gower prey–predator model, the density of prey can influence the carrying capacity of predators such that the density of predators obeys a logistic

[1]Corresponding author.

Table 1. Parameters in model (2), where N represent the number of individual per unit area.

Parameter	Interpretation	Unit
K	Carrying capacity of the prey	N
r_1	Natural growth rate of the prey	time^{-1}
r_2	Natural growth rate of the predator	time^{-1}
b_1	The maximum value of the per capita reduction rate of the prey	time^{-1}
b_2	The maximum value of the per capita reduction rate of the predator	time^{-1}
m_1	Environment protection to the prey	N
m_2	Environment protection to the predator	N

dynamics with a changing capacity proportional. Collings [7] highlights that the Leslie–Gower prey–predator model is sufficient in population dynamics because it can avoid the biological control paradox of classical prey–predator models—a prey density is low in a stable coexistence equilibrium. The modified Leslie–Gower predator–prey model is proposed as

$$\frac{\mathrm{d}U}{\mathrm{d}T} = r_1 U\left(1 - \frac{U}{K}\right) - \frac{b_1 UV}{U + m_1},$$
$$\frac{\mathrm{d}V}{\mathrm{d}T} = r_2 V\left(1 - \frac{b_2 V}{U + m_2}\right),$$

(1)

where U and V separately stand for the total numbers of preys and predators, all parameters are positive constants and their interpretations are described in Table 1.

The distributions of prey and predators are not homogeneous in real world. Thus, we introduce the diffusive terms into model (1), which describe the movement of preys and predators, and obtain the following modified Leslie–Gower reaction–diffusion model:

$$\frac{\partial U}{\partial T} = d_1 \frac{\partial^2 U}{\partial X^2} + r_1 U\left(1 - \frac{U}{K}\right) - \frac{b_1 UV}{U + m_1},$$
$$\frac{\partial V}{\partial T} = d_2 \frac{\partial^2 V}{\partial X^2} + r_2 V\left(1 - \frac{b_2 V}{U + m_2}\right),$$

(2)

where d_1 and d_2 are diffusion rate of the prey and predators, respectively.

In recent years, many researchers have investigated the modified Leslie–Gower predator–prey model (1) and its reaction–diffusion case [1, 2, 14, 15, 25, 26, 29, 33]. By using the perturbation methods, they derived some interesting conclusions such as the stability of equilibriums, bifurcations, travelling waves, periodic solutions and so on.

For mathematical simplicity, using the following scaling transformations

$$T = \frac{t}{r_1}, \qquad X = \sqrt{\frac{1}{r_1}}x, \qquad U = Ku, \qquad V = \frac{r_1 K}{b_1}v,$$
$$\delta = \frac{r_2}{r_1}, \qquad \bar{m}_1 = \frac{m_1}{K}, \qquad \bar{m}_2 = \frac{m_2}{K}, \qquad b = \frac{b_2 r_1}{b_1}$$

and denoting $\bar{m}_1$ and $\bar{m}_2$ by m_1 and m_2, we can get nondimensional model (2) as

$$
\begin{aligned}
\frac{\partial u}{\partial t} &= d_1 \frac{\partial^2 u}{\partial x^2} + u(1-u) - \frac{uv}{u+m_1}, \\
\frac{\partial v}{\partial t} &= d_2 \frac{\partial^2 v}{\partial x^2} + \delta v \left(1 - \frac{bv}{u+m_2} \right).
\end{aligned}
\tag{3}
$$

We study model (3) under assumption that the diffusion rates of predators and prey are similar and sufficiently small and prey grow much faster than predators. It is clear that this assumption is reasonable such as hares and coyotes. In this article, we mainly investigate the travelling waves and periodic solutions of model (3). Hence, using the travelling wave transformation $\tilde{\xi} = x - ct$ [9, 10], we get

$$
\begin{aligned}
-c\frac{du}{d\tilde{\xi}} &= d_1 \frac{d^2 u}{d\tilde{\xi}^2} + u(1-u) - \frac{uv}{u+m_1}, \\
-c\frac{dv}{d\tilde{\xi}} &= d_2 \frac{d^2 v}{d\tilde{\xi}^2} + \delta v \left(1 - \frac{bv}{u+m_2} \right),
\end{aligned}
\tag{4}
$$

where c stands for the velocity of travelling waves. Note that the solution of (4) with $c = 0$ represents standing waves, which is not our main focus in this article. Since system (4) is invariant under transformation $(\tilde{\xi}, c) \to (-\tilde{\xi}, -c)$, then we only need to consider the case $c > 0$. Furthermore, in this paper, we are keen on the travelling waves with $c > 1$, which means the velocity c is larger than the week diffusion rate d_1 and d_2. Hence, by transform $\xi = \tilde{\xi}/c$, the equivalent system of (4) reads

$$
\begin{aligned}
-\frac{du}{d\xi} &= \frac{d_1}{c^2} \frac{d^2 u}{d\xi^2} + u(1-u) - \frac{uv}{u+m_1}, \\
-\frac{dv}{d\xi} &= \frac{d_2}{c^2} \frac{d^2 v}{d\xi^2} + \delta v \left(1 - \frac{bv}{u+m_2} \right).
\end{aligned}
\tag{5}
$$

Under our assumption, we introduce following new notations:

$$
\epsilon = \frac{d_1}{c^2}, \qquad d = \frac{d_2}{d_1}, \qquad u_1 = u, \qquad u_2 = \frac{du}{d\xi}, \qquad v_1 = v, \qquad v_2 = \frac{dv}{d\xi},
$$

and we rewrite (5) as a singularly perturbed system

$$
\begin{aligned}
\frac{du_1}{d\xi} &= u_2, & \epsilon \frac{du_2}{d\xi} &= -u_2 + \frac{u_1 v_1}{u_1 + m_1} - u_1(1-u_1), \\
\frac{dv_1}{d\xi} &= v_2, & \epsilon \frac{dv_2}{d\xi} &= -\frac{1}{d} v_2 - \frac{\delta}{d} v_1 \left(1 - \frac{bv_1}{u_1 + m_2} \right),
\end{aligned}
\tag{6}
$$

where ϵ and δ are sufficiently small parameters, and ξ is called the slow variable. Furthermore, we assume that ϵ and δ satisfy $0 < \epsilon \ll \delta \ll 1$.

For the fast variable $\zeta = \xi/\epsilon$, we get

$$
\begin{aligned}
\frac{du_1}{d\zeta} &= \epsilon u_2, & \frac{du_2}{d\zeta} &= -u_2 + \frac{u_1 v_1}{u_1 + m_1} - u_1(1 - u_1), \\
\frac{dv_1}{d\zeta} &= \epsilon v_2, & \frac{dv_2}{d\zeta} &= -\frac{1}{d} v_2 - \frac{\delta}{d} v_1 \left(1 - \frac{b v_1}{u_1 + m_2} \right).
\end{aligned}
\tag{7}
$$

Note that systems (6) and (7) are separately called the slow system and the fast system, and their dynamics are equivalent.

The slow-fast system is an important component in biological models and investigated by many investigators, who obtained some new dynamics. For prey–predator model, Ambrosio et al. [3] and Zhang and Wang [32] separately studied the relaxation oscillation cycle of system (1) with one small parameter. In [20], Li and Zhu investigated the canard cycles and relaxation oscillation cycle of a slow-fast prey–predator system with Holling III and IV response functions. Furthermore, in [28], Shen investigated the dynamics of similar model with Holling IV response function. Atabaigi and Barati [4] also investigate the relaxation oscillation cycle and canard explosion phenomenon of a slow-fast Holling–Tanner model with Holling IV response function. Indeed, Zhang and Wang [31] studied the dynamics of a slow-fast Holling–Tanner model with Holling III response function. For high dimension model, Liu, Xiao and Yi [23] considered the relaxation oscillation cycle of a slow-fast prey-predator model with one prey and two competing predators, and Shen, Hsu and Yang [27] studied the dynamics of a slow-fast intraguild predation model. For reaction–diffusion cases, Ducrot, Liu and Magal [11] studied the large speed traveling waves for the diffusive Rosenzweig–MacArthur predator–prey model, and Cai, Ghazaryan and Manukian [5] studied the travelling waves for the diffusive Rosenzweig–MacArthur and Holling–Tanner models with two small parameters. Furthermore, the geometric singular perturbation theory is an useful analysis method in these paper.

Recently, the geometric singular perturbation theory has been a main method in the analysis of a slow-fast system and it contains many mathematical tools such as the Fenichel theory [12, 18], the exchange lemma [21, 22], the blow-up method [16, 17] and the entry-exit function [8, 30] and so on. Whereas, the foundation of geometric singular perturbation theory is the Fenichel theory about locally invariant manifolds. Its main conclusion is that, when $0 < \epsilon \ll 1$, there is a locally invariant slow manifold M_ϵ in $O(\epsilon)$-neighborhood of a normally hyperbolic sub-manifold of the critical manifold M_0.

In this article, we will apply the methods and conclusions in geometric singular theory to analyse (6) and (7). We obtain the existence of heteroclinic orbits corresponding to travelling waves and canard cycles and relaxation oscillation cycle corresponding to periodic solutions of system (3). Furthermore, compared with the result for two-dimensional space in [3, 32], we analyse the canard cycles and relaxation oscillation cycle of the four-dimensional slow-fast system (6) with two small parameters. Indeed, we also illustrate the canard explosion phenomenon which is the changing process from a small limit cycle in the singular Hopf bifurcation to the relaxation oscillation cycle.

The rest of this article is organized as follows. In Section 2, we reduce system (6) to the plane (u_1, v_1). We analyse the existence of travelling waves in Section 3 and prove the

existence of canard explosion phenomenon and relaxation oscillation cycle in Section 4. Finally, we give the conclusion in Section 5.

2   Equilibriums and critical manifold

Under our assumption $0 < \epsilon \ll \delta \ll 1$, it is clear that system (6) is a multiscale slow-fast system. Thus, using the method in [5, 13, 24], we reduce the multiscale slow-fast system (6) twice by the geometric singular perturbation. The first reduction is respect to smaller parameter ϵ, and the second is respect to δ.

For $\epsilon = 0$, the degenerate system of (6) reads

$$\frac{\mathrm{d}u_1}{\mathrm{d}\xi} = u_2, \qquad 0 = -u_2 + \frac{u_1 v_1}{u_1 + m_1} - u_1(1 - u_1),$$
$$\frac{\mathrm{d}v_1}{\mathrm{d}\xi} = v_2, \qquad 0 = -\frac{1}{d}v_2 - \frac{\delta}{d}v_1\left(1 - \frac{bv_1}{u_1 + m_2}\right),$$

and we have the critical manifold

$$M_{\epsilon=0} = \left\{(u_1, u_2, v_1, v_2) \mid u_2 = \frac{u_1 v_1}{u_1 + m_1} - u_1(1 - u_1),\ v_2 = -\delta v_1\left(1 - \frac{bv_1}{u_1 + m_2}\right)\right\},$$

which is the set of equilibriums for the layer system of (7) as

$$\frac{\mathrm{d}u_1}{\mathrm{d}\zeta} = 0, \qquad \frac{\mathrm{d}u_2}{\mathrm{d}\zeta} = -u_2 + \frac{u_1 v_1}{u_1 + m_1} - u_1(1 - u_1),$$
$$\frac{\mathrm{d}v_1}{\mathrm{d}\zeta} = 0, \qquad \frac{\mathrm{d}v_2}{\mathrm{d}\zeta} = -\frac{1}{d}v_2 - \frac{\delta}{d}v_1\left(1 - \frac{bv_1}{u_1 + m_2}\right).$$

It is easy to verify each point of $M_{\epsilon=0}$ has eigenvalues -1 and $-1/d$ besides the two zero eigenvalues. Hence, the critical manifold $M_{\epsilon=0}$ is normally hyperbolic and attracting based on the Fenichel theory [12, 18]. Furthermore, the dynamics in critical manifold $M_{\epsilon=0}$ are defined by the limiting system

$$\frac{\mathrm{d}u_1}{\mathrm{d}\xi} = \frac{u_1 v_1}{u_1 + m_1} - u_1(1 - u_1),$$
$$\frac{\mathrm{d}v_1}{\mathrm{d}\xi} = \delta v_1\left(\frac{bv_1}{u_1 + m_2} - 1\right), \tag{8}$$

which is a slow-fast system respect to small parameter $0 < \delta \ll 1$.

Based on the geometric singular perturbation theory [6, 18], there is a two dimensional stable slow manifold M_ϵ for $\epsilon > 0$, which is viewed as a ϵ-order perturbation of the critical manifold $M_{\epsilon=0}$, i.e., $M_\epsilon = M_{\epsilon=0} + O(\epsilon)$. Furthermore, the flows on M_ϵ are govern by the δ-perturbation of system (8). Hence, we only need to investigate system (8).

In order to simplify our analysis processes, we make the following scale transformation:

$$\mathrm{d}\xi = -(u_1 + m_1)(u_1 + m_2)\mathrm{d}\xi'. \tag{9}$$

We still denote ξ' by ξ. Hence, system (8) reads

$$\frac{\mathrm{d}u_1}{\mathrm{d}\xi} = u_1(u_1 + m_2)\big[(1 - u_1)(u_1 + m_1) - v_1\big] \triangleq u_1 f(u_1, v_1, \eta),$$
$$\frac{\mathrm{d}v_1}{\mathrm{d}\xi} = \delta v_1(u_1 + m_1)\big[(u_1 + m_2) - bv_1\big] \triangleq \delta g(u_1, v_1, \eta),$$

$$(10)$$

where $\eta = (m_1, m_2, b)$. Note that the orbit direction of system (10) is reversed to that of system (8) because of the transformation (9) and $(u_1 + m_1)(u_1 + m_2) > 0$. Furthermore, system (10) has a invariant region $\{(u_1, v_1) \mid 0 \leqslant u_1 \leqslant 1, v_1 \geqslant 0\}$.

It is easy to see that system (10) is a slow-fast system with respect to fast variable ξ. Hence, rescaling $\tau = \delta\xi$, we get the slow system of (10) as

$$\delta\frac{\mathrm{d}u_1}{\mathrm{d}\tau} = u_1(u_1 + m_2)\big[(1 - u_1)(u_1 + m_1) - v_1\big],$$
$$\frac{\mathrm{d}v_1}{\mathrm{d}\tau} = v_1(u_1 + m_1)\big[(u_1 + m_2) - bv_1\big],$$

$$(11)$$

where τ is the slow variable. Similarly, let $\delta \to 0$ in system (10) and (11). We obtain the degenerate system

$$0 = u_1(u_1 + m_2)\big[(1 - u_1)(u_1 + m_1) - v_1\big],$$
$$\frac{\mathrm{d}v_1}{\mathrm{d}\tau} = v_1(u_1 + m_1)\big[(u_1 + m_2) - bv_1\big],$$

$$(12)$$

which is defined on the critical manifold

$$M_{\epsilon=0,\,\delta=0} = M^0_{\epsilon=0,\,\delta=0} \cup M^p_{\epsilon=0,\,\delta=0}$$
$$= \big\{(u_1, v_1) \mid u_1 = 0\big\} \cup \big\{(u_1, v_1) \mid v_1 = h_1(u_1), \, 0 \leqslant u_1 \leqslant 1\big\}$$

with $v_1 = h_1(u_1) = (1 - u_1)(u_1 + m_1)$, and the layer system

$$\frac{\mathrm{d}u_1}{\mathrm{d}\xi} = u_1(u_1 + m_2)\big[(1 - u_1)(u_1 + m_1) - v_1\big], \qquad \frac{\mathrm{d}v_1}{\mathrm{d}\xi} = 0. \qquad (13)$$

Clearly, the critical manifold $M_{\epsilon=0,\,\delta=0}$ consists of four normally hyperbolic submanifolds

$$M^{0r}_{\epsilon=0,\,\delta=0} = \big\{(u_1, v_1) \mid u_1 = 0, \, 0 \leqslant v_1 < m_1\big\},$$
$$M^{0a}_{\epsilon=0,\,\delta=0} = \big\{(u_1, v_1) \mid u_1 = 0, \, v_1 > m_1\big\},$$
$$M^{pr}_{\epsilon=0,\,\delta=0} = \Big\{(u_1, v_1) \mid 0 \leqslant u_1 < \frac{1 - m_1}{2}, \, v_1 = h_1(u_1)\Big\},$$
$$M^{pa}_{\epsilon=0,\,\delta=0} = \Big\{(u_1, v_1) \mid \frac{1 - m_1}{2} < u_1 \leqslant 1, \, v_1 = h_1(u_1)\Big\}.$$

Furthermore, it is clear that $M^{0a}_{\epsilon=0,\,\delta=0}$ and $M^{pa}_{\epsilon=0,\,\delta=0}$ are attracting; $M^{0r}_{\epsilon=0,\,\delta=0}$ and $M^{pr}_{\epsilon=0,\,\delta=0}$ are repelling; $(0, m_1)$ is a turning point, and $M = (u_M, v_M) = ((1 - m_1)/2,$ $((1 + m_1)/2)^2)$ is a generic fold point.

Through a straight calculation, we can get the following theorem about the existence and stability of equilibriums of system (10).

Theorem 1. *For system* (10)*, the following conclusions hold*:

(i) *System* (10) *has three trivial equilibriums* $A_1(0, 0)$, $A_2(0, m_2/b)$ *and* $A_3(1, 0)$. *Furthermore,* $A_1(0, 0)$ *is a unstable node and* $A_2(0, m_2/b)$ *and* $A_3(1, 0)$ *are saddle points if* $m_2 < bm_1$.

(ii) *If* $m_2 < bm_1$*, system* (10) *has a unique positive equilibrium* $A^*(u^*, v^*)$ *satisfying* $v^* = h_1(u^*) = h_2(u^*)$*, where* $h_2(u_1) = (u_1 + m_2)/b$*. Furthermore,* $A^*(u^*, v^*)$ *is a stable node located in the right branch of function* $v = h_1(u)$ *for* $\eta \in D_1$ *and is an unstable node located in the left branch of function* $v = h_1(u)$ *for* $\eta \in D_2$; *see Fig.* 1. *Here*

$$D_1 = \left\{ (m_1, m_2, b) \,\bigg|\, m_1 < 1, \ m_2 < b\left(\frac{1 + m_1}{2}\right)^2 - \frac{1 - m_1}{2}, \ m_2 < bm_1 \right\}$$

and

$$D_2 = \left\{ (m_1, m_2, b) \,\bigg|\, m_1 < 1, \ b\left(\frac{1 + m_1}{2}\right)^2 - \frac{1 - m_1}{2} < m_2 < bm_1 \right\}.$$

Note that the equilibriums in Theorem 1 are the spatially homogeneous equilibriums of model (3). In what follows, we will investigate the travelling waves about spatially homogeneous equilibrium A^* and the periodic solutions of model (3). In other words, we will study the heteroclinic orbits about equilibrium A^*, canard cycles and relaxation oscillation cycle of system (10).
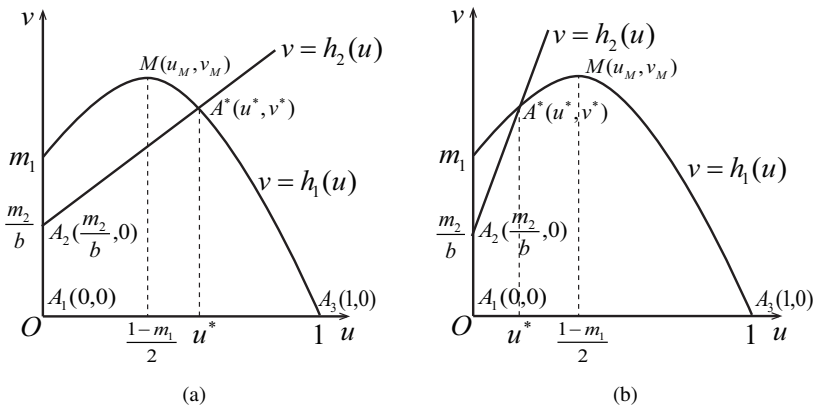
Figure 1. The location of positive equilibrium $A^*(u^*, v^*)$.

3   Travelling waves analysis

In this section, we investigate the heteroclinic orbits of system (10) with $\eta \in D_1$, where $A^*(u^*, v^*)$ is located in the right branch of function $v_1 = h_1(u_1)$.

On $M^p_{\epsilon=0,\,\delta=0}$, system (12) is reduced to

$$\frac{\mathrm{d}u_1}{\mathrm{d}\tau} = \frac{b(u_1 + m_1)^2(u_1 - 1)(h_2(u_1) - h_1(u_1))}{2u_1 + m_1 - 1}, \tag{14}$$

which allows assert that the value of u_1 decreases on segment $(0, u_M)$ and $(u^*, 1)$ and increases on segment (u_M, u^*). Hence, system (14) has a stable equilibrium $u_1 = u^*$ corresponding to $A^*(u^*, v^*)$ and an unstable equilibrium $u_1 = 1$ corresponding to $A_3(1, 0)$. Indeed, there exists a singular orbit from $A_3(1, 0)$ to $A^*(u^*, v^*)$.

With similar analysis, we can get the dynamics of (12) on $M^0_{\epsilon=0,\,\delta=0}$. Hence, the dynamics of (10) and (11) with $\delta = 0$ are shown in Fig. 2(a). Moreover, we have the following lemma about the heteroclinic orbits of positive equilibrium $A^*(u^*, v^*)$.

Lemma 1. *For any fixed $\eta = (m_1, m_2, b) \in D_1$, there is $\delta_0 = \delta(\eta) > 0$ such that for all $0 < \delta < \delta_0$, the following conclusions hold:*

   (i) *System (11) has a heteroclinic orbit from saddle $A_3(1, 0)$ to stable node $A^*(u^*, v^*)$ and a heterocilinc orbit from unstable node $A_1(0, 0)$ to saddle $A_2(0, m_2/b)$.*

   (ii) *System (11) has a heteroclinic orbit from saddle $A_2(0, m_2/b)$ to stable node $A^*(u^*, v^*)$.*

   (iii) *System (11) has infinitely many heteroclinic orbits from unstable node $A_0(0, 0)$ to stable node $A^*(u^*, v^*)$.*

Proof. (i) Since $M^{pa}_{\epsilon=0,\,\delta=0}$ is a normally hyperbolic manifold, then, based on the Finichel theory [12, 18], there is a slow manifold $M^{pa}_{\epsilon=0,\,\delta}$ in the $O(\delta)$-neighborhood of $M^{pa}_{\epsilon=0,\,\delta=0}$ when δ is sufficiently small. Furthermore, the equilibriums $A^*(u^*, v^*)$ and $A_3(1, 0)$ lie in the slow manifold $M^{pa}_{\epsilon=0,\,\delta}$, and the flows on $M^{pa}_{\epsilon=0,\,\delta}$ can be viewed as δ-order perturbation of the flows determined by (14). For (11) with $\delta = 0$, it is clear that the stable manifold of $A^*(u^*, v^*)$ transversally intersects the unstable manifold of $A_3(1, 0)$ based on dimension counting. Indeed, this means that the singular orbit between $A^*(u^*, v^*)$ and $A_3(1, 0)$ persists under perturbation $0 < \delta \ll 1$.

Furthermore, we can similarly prove the heteroclinic orbit between unstable node $A_1(0, 0)$ and saddle point $A_2(0, m_2/b)$.

(ii) Clearly, there exists a singular orbit from $A_2(0, m_2/b)$ to $A^*(u^*, v^*)$ because of $W^s(M^{pa}_{\epsilon=0,\,\delta=0}) \cap W^u_0(A_2) \neq \emptyset$. Note that the intersection of $W^u(M^{pa}_{\epsilon=0,\,\delta=0})$ and $W^u_0(A_2)$ is transverse by dimension counting. According to the Finechel theory [12, 18], $W^u(M^{pa}_{\epsilon=0,\,\delta=0})$ is perturbed to two dimensional stable manifold $W^s_\delta(A^*)$, and $W^u_0(A_2)$ is perturbed to the unstable manifold $W^u_\delta(A_2)$ of saddle $A_2(0, m_2/b)$. Furthermore, the intersection of $W^s_\delta(A^*)$ and $W^u_\delta(A_2)$ is persist because of the transverse intersection $W^s(M^{pa}_{\epsilon=0,\,\delta=0}) \cap W^u_0(A_2)$.

(iii) The proof process is similar to that of (ii).   □
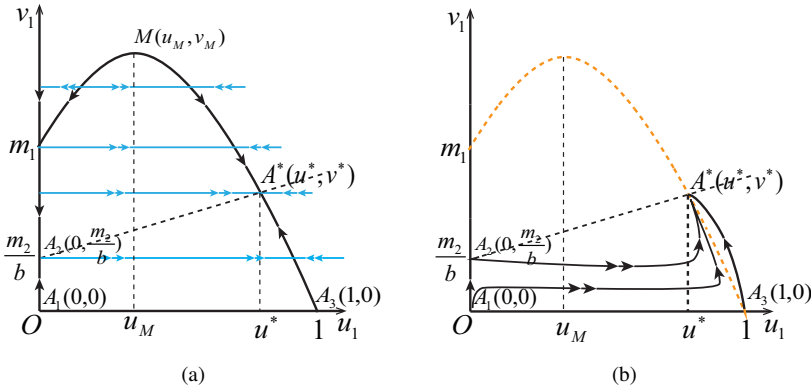
Figure 2. (a) The dynamics of systems (10) and (11) with $\delta = 0$; (b) the heteroclinic orbits of system (10) with $0 < \delta \ll 1$.

Note that the picture of Lemma 1 is shown in Fig. 2(b). Furthermore, for system (8), we have the following remark.

Remark 1. Since the transformation (9), the flows of system (8) are reversed to that of system (10). Hence, the positive equilibrium $A^*(u^*, v^*)$ of system (8) is unstable, and the heteroclinic orbits in Lemma 1 are also heteroclinic orbits of system (8) with oppositive direction.

Since $M_{\epsilon=0}$ is normally hyperbolic attracting manifold, then there exists a attracting slow manifold M_ϵ near $M_{\epsilon=0}$ for sufficiently small $\epsilon > 0$. Moreover, the heteroclinic orbits in Lemma 1 are transversal, then they persist on slow manifold M_ϵ. Indeed, according to Remark 1, we have the following theorem for system (6).

Theorem 2. *For any fixed $\eta = (m_1, m_2, b) \in D_1$, there exist $\delta_0 = \delta_0(\eta) > 0$ and $\epsilon_0 = \epsilon_0(\eta, \delta) > 0$ such that for all $0 < \delta < \delta_0$ and $0 < \epsilon < \epsilon_0$, the following conclusions hold*:

  (i) *System (6) has a heteroclinic orbit from saddle $(u^*, 0, v^*, 0)$ to saddle $(1, 0, 0, 0)$ and a heterocilinc orbit from saddle $(0, 0, m_2/b, 0)$ to stable node $(0, 0, 0, 0)$.*

  (ii) *System (6) has a heteroclinic orbit from saddle $(u^*, 0, v^*, 0)$ to saddle $(0, 0, m_2/b, 0)$.*

  (iii) *System (6) has infinite heteroclinic orbits from saddle $(u^*, 0, v^*, 0)$ to stable node $(0, 0, 0, 0)$.*

Note that these heteroclinic orbits in Theorem 2 are corresponded to different travelling waves of model (3). The biological explanation is that, if $\eta = (m_1, m_2, b) \in D_1$, the predators will be eventual extinction, and the prey will extinct or attach the carrying capacity. Furthermore, we give the following example to verify our conclusions.

Example 1. Set $\delta = 0.02$, $m_1 = 0.6$, $m_2 = 0.1$ and $b = 0.8$ in (8). It is clear that there exist the positive equilibrium $A^*(0.38471, 0.60588)$ and the heteroclinic orbits in Lemma 1; see Fig. 3. The travelling waves of model (3) are shown in Fig. 4, which correspond to the heteroclinic orbits in Theorem 2.
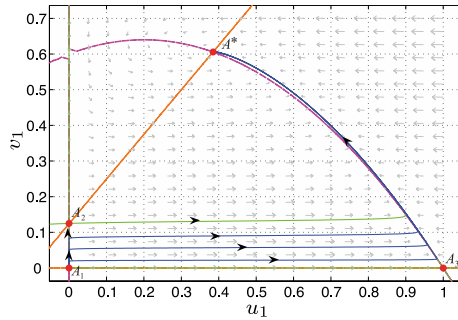
Figure 3. The heteroclinic orbits of system (10) with $\delta = 0.02$, $m_1 = 0.6$, $m_2 = 0.1$ and $b = 0.8$.
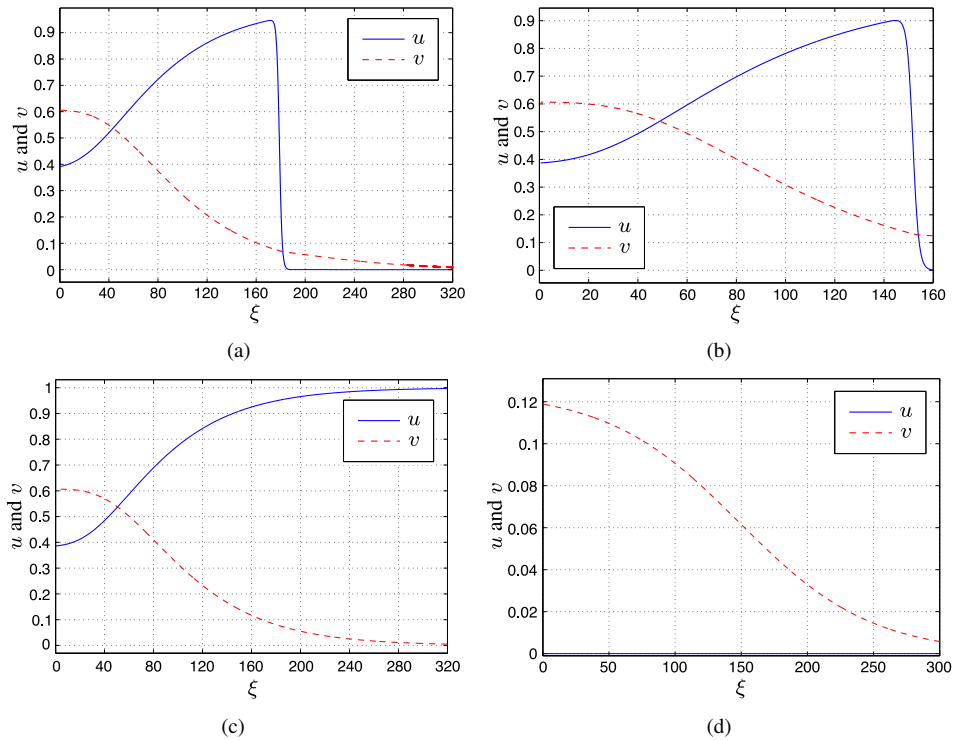
Figure 4. The travelling waves of model (3) with $\delta = 0.02$, $m_1 = 0.6$, $m_2 = 0.1$ and $b = 0.8$, where (a) A^* to A_1, (b) A^* to A_2, (c) A^* to A_3 and (d) A_1 to A_2.

4 Periodic solutions analysis

In this section, we mainly investigate the existence of periodic solutions for model (3) with sufficiently small parameters $0 < \epsilon \ll \delta \ll 1$. This means that we are interested in

the periodic orbits of the slow-fast system (6). However, the canard explosion is the most important periodic orbit phenomenon in a slow-fast system. In [16, 17], this phenomenon is described as a small cycle arising in a singular Hopf bifurcation grows through a sequence canard cycles without head and canard cycles with head to a relaxation oscillation cycle. Canard cycles come from the perturbation of a singular slow-fast cycles, which consist of the attracting and repelling part of critical manifold $M_{\epsilon=0,\,\delta=0}$ and the fast orbits of layer system (13). Hence, we will give some results about the canard cycles, canard explosion phenomenon and relaxation oscillation cycle in this section.

To begin with, we give a result about the exit-entry function of system (10).

Lemma 2. *For system* (10) *and fixed* $v^0 \in (m_1, +\infty)$, *there is an unique* $\hat{v}^* \in (m_2/b, m_1)$ *such that*

$$\int_{v^0}^{\hat{v}^*} \frac{f(0, v_1, \eta)}{g(0, v_1, \eta)} \, \mathrm{d}v_1 = 0. \tag{15}$$

Proof. Let

$$I(\hat{v}) = \int_{v^0}^{\hat{v}} \frac{f(0, v_1, \eta)}{g(0, v_1, \eta)} \, \mathrm{d}v_1 = \int_{v^0}^{\hat{v}} \frac{\frac{v_1}{m_1} - 1}{v_1\left(\frac{bv_1}{m_2} - 1\right)} \, \mathrm{d}v_1.$$

It is clear that $\lim_{\hat{v} \to m_2/b} I(\hat{v}) = +\infty$ and $I(m_1) < 0$. Indeed, we also have $I'(\hat{v}) < 0$, $\hat{v} \in (m_2/b, m_1)$. Hence, we can conclude that there is an unique $\hat{v}^* \in (m_2/b, m_1)$ such that $I(\hat{v}^*) = 0$. □

4.1 Canard cycle and canard explosion

In order to find the canard cycles, we need to ensure that the generic fold point $M(u_M, v_M)$ satisfies the canard point condition, i.e., $g(u_M, v_M, \eta) = 0$, which means that the equilibrium of degenerate system (12) coincides with $M(u_M, v_M)$; see Fig. 5(a). With a similar analysis, we obtain the dynamics of (10) and (11) with $\delta = 0$; see Fig. 5(b).

Hence, we can construct a family of singular slow-fast cycles $\Gamma_0^c(s)$ (see Fig. 6(a)) as

$$\Gamma_0^c(s) = \left\{(u_1, v_1) \mid v_1 = h_1(u_1), \; u_1 \in [\alpha(s), \omega(s)]\right\}$$
$$\cup \left\{(u_1, v_1) \mid v_1 = v_M - s, \; u_1 \in [\alpha(s), \omega(s)]\right\},$$

where $s \in (0, v_M - m_1)$, and $\alpha(s), \omega(s)$ are two roots of the equation $h_1(u_1) = v_M - s$, and a family of singular slow-fast cycles $\Gamma_0^{ch}(s)$ (see Fig. 6(b)) as

$$\Gamma_0^{ch}(s) = \left\{(u_1, v_1) \mid v_1 = h_1(u_1), \; u_1 \in [\alpha(s), \omega(s)]\right\}$$
$$\cup \left\{(u_1, v_1) \mid v_1 = v_M - s, \; u_1 \in [0, \alpha(s)]\right\}$$
$$\cup \left\{(u_1, v_1) \mid v_1 \in [\bar{v}(s), v_M - s], \; u_1 = 0\right\}$$
$$\cup \left\{(u_1, v_1) \mid v_1 = \bar{v}(s), \; u_1 \in [0, \omega(s)]\right\},$$
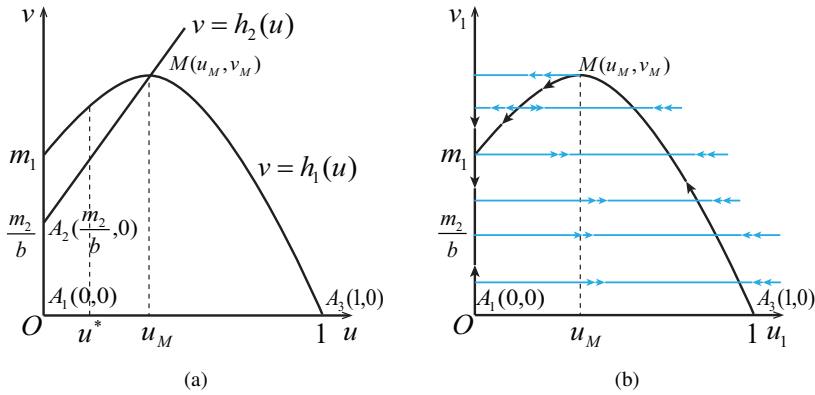
Figure 5. (a) Canard point $M(u_M, v_M)$; (b) the dynamics of (10) and (11) with $\delta = 0$ when $M(u_M, v_M)$ is a canard point.
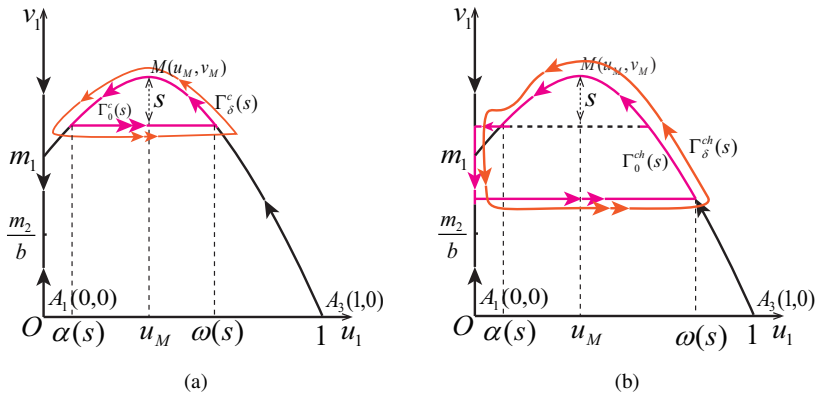
Figure 6. (a) Canard cycles without head, where the pink line is a singular slow-fast cycle $\Gamma_0^c(s)$, and the orange line is a canard cycle without head $\Gamma_\delta^c(s)$ near $\Gamma_0^c(s)$; (b) canard cycles with head, where the pink line is a singular slow-fast cycle $\Gamma_0^{ch}(s)$, and the orange line is a canard cycle with head $\Gamma_\delta^{ch}(s)$ near $\Gamma_0^{ch}(s)$.

where $s \in (0, v_M - m_1)$, $\bar{v}(s)$ defined by (15) in Lemma 2 when $v^0 = v_M - s$. $\alpha(s)$ is the smaller root of the equation $h_1(u_1) = v_M - s$, and $\omega(s)$ is the larger root of the equation $h_1(u_1) = \bar{v}(s)$.

For the dynamics of system (10) near canard point $M(u_M, v_M)$, we align $M(u_M, v_M)$ to origin point by transformation $\bar{u} = u_1 - u_M$ and $\bar{v} = v_1 - v_M$ and denote $(\bar{u}, \bar{v})$ by (u_1, v_1). Then we rewrite system (10) as

$$
\begin{aligned}
\frac{du_1}{d\xi} &= -v_1\big[u_M(u_M + m_2) + O(u_1)\big] \\
&\quad - u_1^2\big[u_M(u_M + m_2) + (2u_M + m_2)u_1 + u_1^2\big], \\
\frac{dv_1}{d\xi} &= \delta\big[P_0 + P_1 u_1 + P_2 u_1^2 + v_1(P_3 + P_4 u_1 + P_5 v_1) + O(3)\big],
\end{aligned}
\tag{16}
$$

where

$$P_0 = (u_M + m_1)v_M(u_M + m_2 - bv_M), \quad P_1 = v_M(m_1 + m_2 + 2u_M - bv_M),$$
$$P_2 = v_M, \qquad\qquad\qquad\qquad\qquad P_3 = (u_M + m_1)(u_M + m_2 - 2bv_M),$$
$$P_4 = m_1 + m_2 + 2u_M - 2bv_M, \qquad P_5 = -b(u_M + m_1).$$

Note that we can choose suitable value of b such that $P_1 > 0$.

In order to use the conclusions in [16, 17], by a straightforward calculation, we can obtain the slow-fast normal form of (16) as

$$\frac{\mathrm{d}u_1}{\mathrm{d}\xi} = -v_1 h_1(u_1, v_1, \lambda, \delta) + u_1^2 h_2(u_1, v_1, \lambda, \delta) + \delta h_3(u_1, v_1, \lambda, \delta),$$
$$\frac{\mathrm{d}v_1}{\mathrm{d}\xi} = \delta\big[u_1 h_4(u_1, v_1, \lambda, \delta) - \lambda h_5(u_1, v_1, \lambda, \delta) + v_1 h_6(u_1, v_1, \lambda, \delta)\big], \tag{17}$$

where

$$h_1(u_1, v_1, \lambda, \delta) = 1 + O(1),$$

$$h_2(u_1, v_1, \lambda, \delta) = 1 - \frac{(2u_M + m_2)P_1^{1/2}u_1}{u_M^{3/2}(u_M + m_2)^{3/2}} + \frac{P_1 u_1^2}{u_M^2(u_M + m_2)^2},$$

$$h_3(u_1, v_1, \lambda, \delta) = 0,$$

$$h_4(u_1, v_1, \lambda, \delta) = 1 - \frac{P_2 u_1}{\sqrt{u_M(u_M + m_2)P_1}},$$

$$h_5(u_1, v_1, \lambda, \delta) = 1,$$

$$h_6(u_1, v_1, \lambda, \delta) = \frac{P_3}{\sqrt{u_M(u_M + m_2)P_1}} - \frac{P_4 u_1}{u_M(u_M + m_2)} - \frac{P_5\sqrt{P_1}v_1}{u_M^{3/2}(u_M + m_2)^{3/2}}$$

and

$$\lambda = \frac{\sqrt{u_M(u_M + m_2)}P_0}{P_1^{3/2}}. \tag{18}$$

Clearly, $\lambda = 0$ implies that $P_0 = 0$, which is equal to $b = (u_M + m_2)/v_M$.

Hence, according to [16, 17], we obtain

$$a_1 = \frac{\partial h_3}{\partial u_1}(0, 0, 0, 0) = 0, \qquad a_2 = \frac{\partial h_1}{\partial u_1}(0, 0, 0, 0) = 0,$$

$$a_3 = \frac{\partial h_2}{\partial u_1}(0, 0, 0, 0) = -\frac{v_M^{1/2}(u_M + m_1)^{1/2}(2u_M + m_2)}{u_M^{3/2}(u_M + m_2)^{3/2}},$$

$$a_4 = \frac{\partial h_4}{\partial u_1}(0, 0, 0, 0) = -\sqrt{\frac{v_M}{u_M(u_M + m_1)(u_M + m_2)}},$$

$$a_5 = h_6(0, 0, 0, 0) = -\sqrt{\frac{(u_M + m_1)(u_M + m_2)}{v_M u_M}}$$

and

$$A = -a_2 + 3a_3 - 2a_4 - 2a_5 = \frac{\hat{A}}{\sqrt{u_M^3(u_M + m_2)^3(1 - u_M)}},$$

where

$$\hat{A} = 2u_M(1 + m_2)(u_M + m_2) - 3v_M(2u_M + m_2).$$

Then the singular Hopf bifurcation curve $\lambda_H(\sqrt{\delta})$ and maximal canard curve $\lambda_c(\sqrt{\delta})$ of system (17) are

$$\lambda_H(\sqrt{\delta}) = -\frac{a_1 + a_5}{2}\delta + O(\delta^{3/2})$$

$$= \frac{1}{2}\sqrt{\frac{(u_M + m_1)(u_M + m_2)}{v_M u_M}}\delta + O(\delta^{3/2})$$

and

$$\lambda_c(\sqrt{\delta}) = -\left(\frac{a_1 + a_5}{2} + \frac{A}{8}\right)\delta + O(\delta^{3/2})$$

$$= \frac{4u_M(u_M + m_2)^2 - \hat{A}}{8\sqrt{u_M^3(u_M + m_2)^3(1 - u_M)}}\delta + O(\delta^{3/2}).$$

Since

$$\lambda'(b) = -\frac{u_M^{1/2}(u_M + m_2)^{1/2}v_M^{1/2}(u_M + m_1)(2m_1 - m_2 + u_M + bv_M)}{2(m_1 + m_2 + 2u_M - bv_M)^{\frac{5}{2}}} < 0,$$

then the equations $\lambda(b) = \lambda_H(\sqrt{\delta})$ and $\lambda(b) = \lambda_c(\sqrt{\delta})$ have unique solutions as

$$b_H(\sqrt{\delta}) = \frac{u_M + m_2}{v_M} - \frac{2}{1 - m_1^2}\delta + O(\delta^{3/2}) \tag{19}$$

and

$$b_c(\sqrt{\delta}) = \frac{u_M + m_2}{v_M} - \frac{4u_M(u_M + m_2)^2 - \hat{A}}{8u_M^2(u_M + m_2)^2(1 - u_M)}\delta + O(\delta^{3/2}). \tag{20}$$

Hence, we have the following theorems about singular Hopf bifurcation from Theorem 3.1 in [17].

Theorem 3. *For fixed $\eta = (m_1, m_2, b) \in D_1 \cup D_2$, suppose the vertex point $M(u_M, v_M)$ of curve $v_1 = h_1(u_1)$ is a canard point, and b and λ satisfy the relationship (18). Then there are $0 < \delta_0 \ll 1$ and $b_0 > 0$ such that for each $0 < \delta < \delta_0$ and $|b - (u_M + m_2)/v_M| < b_0$, system (16) has unique positive equilibrium $A^*(u^*, v^*)$ in the small neighborhood of canard point $M(u_M, v_M)$ and $A^*(u^*, v^*) \to M(u_M, v_M)$ as $(\delta, b) \to (0, (u_M + m_2)/v_M)$. Furthermore, $A^*(u^*, v^*)$ is stable with $b > b_H(\sqrt{\delta})$ and unstable with $b < b_H(\sqrt{\delta})$, where $b_H(\sqrt{\delta})$ is shown in (19). So a Hopf bifurcation occurs when b passes through $b_H(\sqrt{\delta})$. It is supercritical if $\hat{A} > 0$ and subcritical if $\hat{A} < 0$.*

Proof. Let η_M be the parameters $\eta = (m_1, m_2, b)$ satisfying $bv_M = u_M + m_2$. Hence, we have

$$f(u_M, v_M, \eta_M) = 0, \qquad g(u_M, v_M, \eta_M) = 0,$$

$$\frac{\partial(uf)}{\partial u}(u_M, v_M, \eta_M) = 0,$$

$$\frac{\partial^2(uf)}{\partial u^2}(u_M, v_M, \eta_M) = -2u_M(u_M + m_2) < 0,$$

$$f_v(u_M, v_M, \eta_M) = -(u_M + m_2) < 0,$$

$$\frac{\partial g}{\partial u}(u_M, v_M, \eta_M) = v_M(u_M + m_1) > 0,$$

$$\frac{\partial g}{\partial b}(u_M, v_M, \eta_M) = -v_M^2(u_M + m_1) < 0.$$

Then the vertex point $M(u_M, v_M)$ is a nondegenerate canard point. Furthermore, system (17) is the normal form of system (10) in the neighborhood of the nondegenerate canard point $M(u_M, v_M)$. Thus, it is clear that the origin point is a nondegenerate canard point of system (17).

According to Theorem 3.1 in [17], for suitable ϵ and λ, there is a equilibrium p_e of system (17) near $(0, 0)$, which satisfy $p_e \to (0, 0)$ as $(\epsilon, \lambda) \to (0, 0)$. Furthermore, there exists a singular Hopf bifurcation curve $\lambda_H(\sqrt{\epsilon})$ such that p_e is stable for $\lambda < \lambda_H(\sqrt{\epsilon})$ and unstable for $\lambda > \lambda_H(\sqrt{\epsilon})$.

Since $\mathrm{d}\lambda/\mathrm{d}b < 0$, then equation $\lambda(b) = \lambda_H(\sqrt{\delta})$ has unique solution $b = b_H(\sqrt{\delta})$, and $\lambda > \lambda_H(\sqrt{\delta})$ is equal to $b < b_H(\sqrt{\delta})$. Hence, we complete the proof. $\qquad\square$

Moreover, from Lemma 2 and Theorems 3.3 and 3.5 in [17], the canard cycles are shown as follows.

Theorem 4. *For fixed $\eta = (m_1, m_2, b) \in D_1 \cup D_2$, suppose the vertex point $M(u_M, v_M)$ of curve $v_1 = h_1(u_1)$ is a canard point, and b and λ satisfy the relationship (18). Then for $s \in (0, v_M - m_1)$ and $0 < \delta \ll 1$, there exists $b = b(s, \sqrt{\delta})$ such that system (16) has a family of canard cycle $\Gamma_\delta^c(s)(\Gamma_\delta^{ch}(s))$ emerges from $\Gamma_0^c(s)(\Gamma_0^{ch}(s))$; see Fig. 6. Moreover, the family $\Gamma_\delta^c(s)(\Gamma_\delta^{ch}(s))$ uniformly converges to $\Gamma_0^c(s)(\Gamma_0^{ch}(s))$ in Hausdorff distance as $\delta \to 0$, and there exists a curve $b_c(\sqrt{\delta})$ given in (20). For $\nu \in (0, 1)$, the canard explosion occurs when $s \in [\delta^\nu, v_M - m_1 - \delta^\nu]$, where*

$$\left| b(s, \sqrt{\delta}) - b_c(\sqrt{\delta}) \right| < \mathrm{e}^{-1/\delta^\nu}.$$

Proof. The proof is omitted because its main idea is similar to that of Theorem 3. $\qquad\square$

Remark 2. Theorem 4 shows that, for $s \in (0, v_M - m_1)$ and $0 < \delta \ll 1$, there exists $b = b(s, \sqrt{\delta})$ such that the singular slow-fast cycles $\Gamma_0^c(s)$ or $\Gamma_0^{ch}(s)$ can be perturbed the canard cycles $\Gamma_\delta^c(s)$ or $\Gamma_\delta^{ch}(s)$ of system (16). Furthermore, the canard explosion occurs when the parameter b changes in a exponential small neighborhood of the maximal canard curve $b_c(\sqrt{\delta})$.
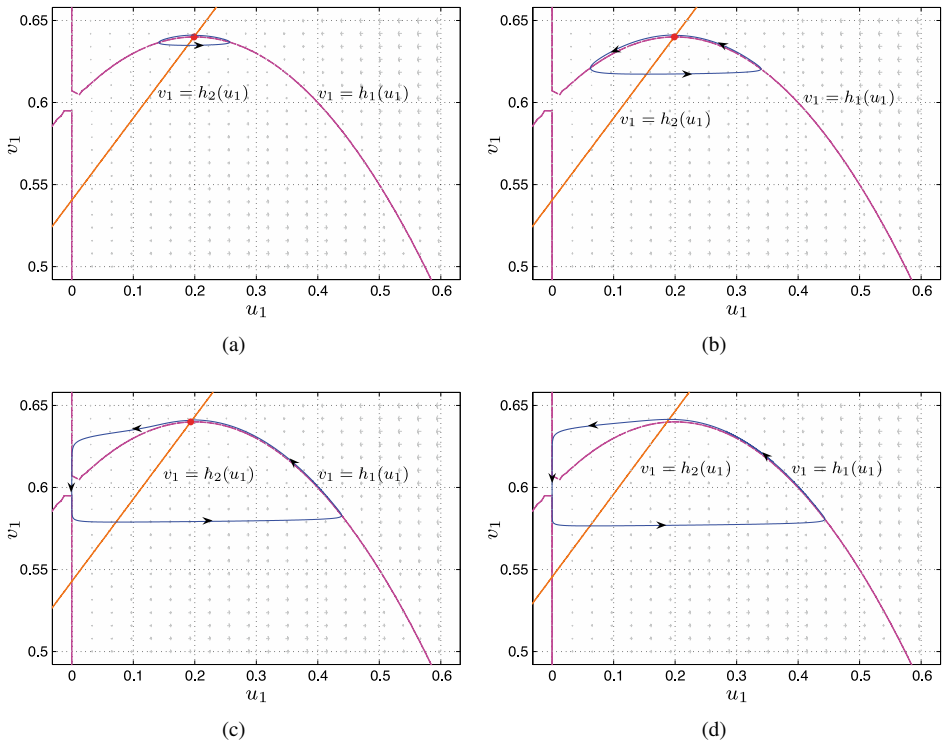
Figure 7. The canard explosion phenomenon of system (10) with $\delta = 0.001$, $m_1 = 0.6$, $m_2 = 1.08$, (a) $\delta = 1.997$; (b) $\delta = 1.995$; (c) $\delta = 1.99$; (d) $\delta = 1.98$.

Indeed, we give an example to show the canard explosion phenomenon as follows.

Example 2. Set $\delta = 0.001$, $m_1 = 0.6$, $m_2 = 1.08$ in (10). It is clear that the value of maximal curve $b_c(\sqrt{\delta}) = 1.9926$, and system (10) has the canard explosion phenomenon; see Fig. 7.

4.2 relaxation oscillation cycle

For $\eta = (m_1, m_2, b) \in D_2$, we have the dynamics of (10) and (11) with $\delta = 0$; see Fig. 8(a).

Let $(\bar{u}^*, \bar{v}^*)$ be the intersection point of $v_1 = \bar{v}^*$ and $v_1 = h_1(u_1)$, where $\bar{v}^*$ defined by (15) in Lemma 2 when $v^0 = v_M$. We denote a singular slow-fast cycle as

$$\Gamma_0 = \big\{(u_1, v_1) \,\big|\, v_1 = h_1(u_1),\ u_M \leqslant u_1 \leqslant \bar{u}^*\big\} \cup \big\{(u_1, v_1) \,\big|\, v_1 = \bar{v}^*,\ 0 \leqslant u_1 \leqslant \bar{u}^*\big\}$$
$$\cup \big\{(u_1, v_1) \,\big|\, \bar{v}^* \leqslant v_1 \leqslant v_M,\ u_1 = 0\big\} \cup \big\{(u_1, v_1) \,\big|\, v_1 = v_M,\ 0 \leqslant u_1 \leqslant u_M\big\},$$

which contains two slow segments and two fast segments; see Fig.8(b). Indeed, according to Theorem 3.2 in [3, 32], we have the following theorem about relaxation oscillation cycle.
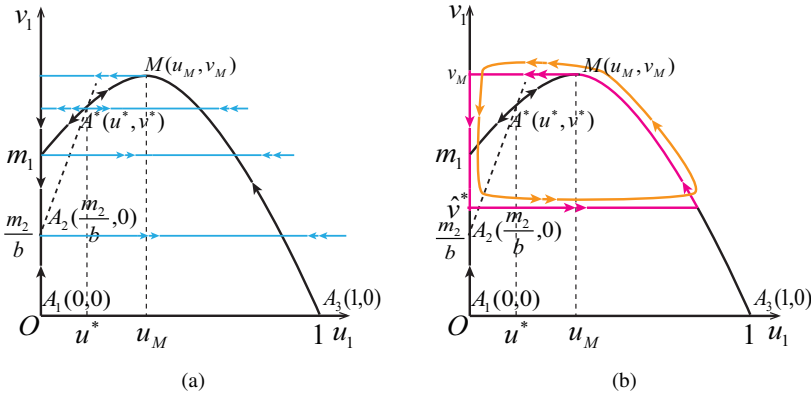
Figure 8. (a) The dynamics of system (10) and (11) with $\delta = 0$; (b) the relaxation oscillation cycle of system (10) with sufficiently small δ, where the pink curve is the singular slow-fast cycle Γ_0, and the orange curve is the relaxation oscillation cycle Γ_ϵ.

Theorem 5. *For any fixed $\eta = (m_1, m_2, b) \in D_2$, there exists $\delta_0 = \delta(\eta)$ such that for $0 < \delta < \delta_0$, system (10) has a unique relaxation oscillation cycle Γ_δ in the $O(\delta)$-neighborhood of Γ_0, which is hyperbolic attracting; see Fig. 8(b). Furthermore, the cycle Γ_δ converges to Γ_0 in the Hausdorff distance as $\delta \to 0$.*

Remark 3. Due to transformation (9), the direction of canard cycles and relaxation oscillation cycle of system (8) is opposite to system (10).

Indeed, we give the following example to show the existence of relaxation oscillation cycle.

Example 3. Set $\delta = 0.001$, $m_1 = 0.6$, $m_2 = 1.08$ and $b = 1.91$ in (10). There exists a relaxation oscillation cycle; see Fig. 9.

Since the critical manifold $M_{\epsilon=0}$ is a normally hyperbolic attracting manifold, then for sufficiently small $0 < \epsilon \ll 1$, there is a slow manifold M_ϵ near $M_{\epsilon=0}$ such that canard cycles and relaxation oscillation cycle persist on it. Hence, we have the following theorem about periodic solution of (3).

Theorem 6. *There exist $\delta_0 = \delta_0(m_1, m_2, b) > 0$ and $\epsilon_0 = \epsilon_0(m_1, m_2, b, \delta) > 0$ such that for all $0 < \delta < \delta_0 \ll 1$ and $0 < \epsilon < \epsilon_0 \ll 1$, the following conclusions hold:*

(i) *For fixed $\eta = (m_1, m_2, b) \in D_1 \cup D_2$, suppose the vertex point $M(u_M, v_M)$ of curve $v_1 = h_1(u_1)$ is a canard point. Then there exists $b = b(s, \sqrt{\delta})$, $s \in (0, v_M - m_1)$, such that model (3) has a family of periodic solutions corresponding to canard cycles.*

(ii) *For fixed $\eta = (m_1, m_2, b) \in D_2$, model (3) has a periodic solution corresponding to relaxation oscillation cycle.*

Note that the picture of a periodic solution of model (3) is given in Fig. 10, which corresponds to the relaxation oscillation cycle shown in Fig. 9.
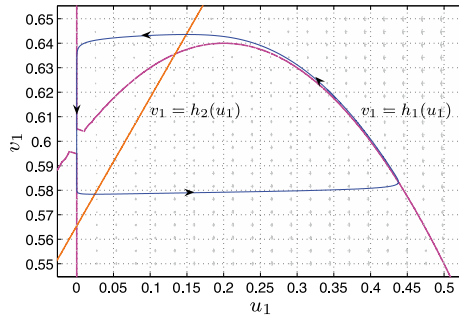
Figure 9. The relaxation oscillation cycle of system (10) with $\delta = 0.001$, $m_1 = 0.6$, $m_2 = 1.08$ and $b = 1.91$.
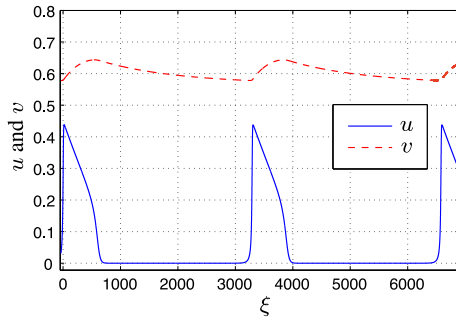
Figure 10. The periodic solution of model (3), which corresponds to the relaxation oscillation cycle shown in Fig. 9.

Remark 4. The periodic solution of system (3) in Fig. 9 means that the predators and preys will coexit since the population of preys sometimes is very low.

5 Conclusion

In this paper, we investigate the diffusive Leslie–Gower prey–predator model (3) under the assumption that both prey and predator diffuse small and prey grows much faster than predator. Thus, this prey–predator model is a singular problem with two small parameters. Using the travelling waves transformation, model (3) is transformed to a multiscale slow-fast system (6) with $0 < \epsilon \ll \delta \ll 1$. Applying the geometric singular perturbation theory, we prove the existence of heteroclinic orbits of system (6) for $\eta \in D_1$, which correspond to the travelling waves of model (3). Indeed, we also prove the existence of relaxation oscillation cycle of system (10) for $\eta \in D_2$ and the canard explosion phenomenon of system (10) when $M(u_M, v_M)$ is a canard point. These periodic cycles imply the existence of periodic solutions of model (3). We also give some numerical examples to show illustration of our theoretical results. Our results have important theoretical significance for the biological control of pests and the conservation of biodiversity. Meanwhile, our method used in this paper can be applied into other similar models.

References

1. W. Abid, R. Yafia, M.A. Aziz-Alaoui, H. Bouhafa, A. Abichou, Global dynamics on a circular domain of a diffusion predator-prey model with modified Leslie–Gower and Beddington-DeAngelis functional type, *Evol. Equ. Control Theory*, **4**(2):115–129, 2015, `https://doi.org/10.3934/eect.2015.4.115`.

2. S. Ai, Y. Du, R. Peng, Traveling waves for a generalized Holling–Tanner predator–prey model, *J. Differ. Equations*, **263**(11):7782–7814, 2017, `https://doi.org/10.1016/j.jde.2017.08.021`.

3. B. Ambrosio, M.A. Aziz-Alaoui, R. Yafia, Canard phenomenon in a slow-fast modified Leslie–Gower model, *Math. Biosci.*, **295**:48–54, 2018, `https://doi.org/10.1016/j.mbs.2017.11.003`.

4. A. Atabaigi, A. Barati, Relaxation oscillations and canard explosion in a predator–prey system of Holling and Leslie types, *Nonlinear Anal., Real World Appl.*, **36**:139–153, 2017, `https://doi.org/10.1016/j.nonrwa.2017.01.006`.

5. H. Cai, A. Ghazaryan, V. Manukian, Fisher-KPP dynamics in diffusive Rosenzweig–MacArthur and Holling–Tanner models, *Math. Model. Nat. Phenom.*, **14**(4):404–425, 2019, `https://doi.org/10.1051/mmnp/2019017`.

6. P.T. Cardin, M.A. Teixeira, Finichel theory for multiple time scale singular perutrbation problems, *SIAM J. Appl. Dyn. Syst.*, **16**(3):1425–1421, 2017, `https://doi.org/10.1137/16M1067202`.

7. J.B. Collings, The effect of the functional response on the bifurcation behavior of a mite predator–prey interaction model, *J. Math. Biol.*, **36**:149–168, 1997, `https://doi.org/10.1007/s002850050095`.

8. P. De Maesschalck, S. Schecter, The entry–exit function and geometric singular perturbation theory, *J. Differ. Equations*, **260**(8):6697–6715, 2016, `https://doi.org/10.1016/j.jde.2016.01.008`.

9. Z.J. Du, J. Li, Geometric singular perturbation analysis to Camassa–Holm Kuramoto–Sivashinsky equation, *J. Differ. Equations*, **306**:418–438, 2022, `https://doi.org/10.1016/j.jde.2021.10.033`.

10. Z.J. Du, J. Liu, Y.L. Ren, Traveling pulse solutions of a generalized Keller–Segel system with small cell diffusion via a geometric approach, *J. Differ. Equations*, **270**:1019–1042, 2021, `https://doi.org/10.1016/j.jde.2020.09.009`.

11. A. Ducrot, Z.H. Liu, P. Magal, Large speed traveling waves for the Rosenzweig–MacArthur predator–prey model with spatial diffusion, *Physica D*, **415**:132730, 14 pp, 2021, `https://doi.org/10.1016/j.physd.2020.132730`.

12. N. Fenichel, Geometric singular perturbation theory for ordinary differential equations, *J. Differ. Equations*, **31**(1):53–98, 1979, `https://doi.org/10.1016/0022-0396(79)90152-9`.

13. A. Ghazaryan, V. Manukian, S. Schecter, Travelling waves in the Holling–Tanner model with weak diffusion, *Proc. R. Soc. Lond., Ser. A*, **471**:20150045, 2015, `https://doi.org/10.1098/rspa.2015.0045`.

14. J.C. Huang, Y.J. Gong, S.G. Ruan, Bifurcation analysis in a predator-prey model with constant-yield predator harvesting, *Discrete Contin. Dyn. Syst., Ser. B*, **18**(8):2101–2121, 2013, `https://doi.org/10.3934/dcdsb.2013.18.2101`.

15. J.C. Huang, S.H. Liu, S.G. Ruan, X.A. Zhang, Bogdanov-Takens bifurcation of codimension 3 in a predator-prey model with constant-yield predator harvesting, *Commun. Pure Appl. Anal.*, **15**(3):1041–1055, 2016, `https://doi.org/10.3934/cpaa.2016.15.1041`.

16. M. Krupa, P. Szmolyan, Extending geometric singular perturbation theory to nonhyperbolic points-fold and canard points in two dimensions, *SIAM J. Math. Anal.*, **33**(2):286–314, 2001, `https://doi.org/10.1137/S0036141099360919`.

17. M. Krupa, P. Szmolyan, Relaxation oscillation and canard explosion, *J. Differ. Equations*, **174**(2):312–368, 2001, `https://doi.org/10.1006/jdeq.2000.3929`.

18. C. Kuehn, *Multiple Time Scale Dynamics*, Appl. Math. Sci., Vol. 191, Springer, Cham, 2015, `https://doi.org/10.1007/978-3-319-12316-5`.

19. P.H. Leslie, Some further notes on the use of matrices in population mathematics, *Biometrika*, **35**:213–245, 1948.

20. C.Z. Li, H.P. Zhu, Canard cycles for predator-prey systems with Holling types of functional response, *J. Differ. Equations*, **254**(2):879–910, 2013, `https://doi.org/10.1016/j.jde.2012.10.003`.

21. W.S. Liu, Exchange lemmas for singular perturbation problems with certain turning points, *J. Differ. Equations*, **167**(1):134–180, 2000, `https://doi.org/10.1006/jdeq.2000.3778`.

22. W.S. Liu, Geometric singular perturbations for multiple turning points: Invariant manifolds and exchange lemmas, *J. Dyn. Differ. Equ.*, **18**:667–691, 2006, `https://doi.org/10.1007/s10884-006-9020-7`.

23. W.S. Liu, D.M. Xiao, Y. Yi, Relaxation oscillations in a class of predator–prey systems, *J. Differ. Equations*, **188**(1):306–331, 2003, `https://doi.org/10.1016/S0022-0396(02)00076-1`.

24. V. Manukian, On traveling waves of Gray–Scott model, *Dyn. Syst.*, **30**(3):270–296, 2015, `https://doi.org/10.1080/14689367.2015.1027177`.

25. W.J. Ni, M.X. Wang, Dynamical properties of a Leslie-Gower prey-predator model with strong Allee effect in prey, *Discrete Contin. Dyn. Syst., Ser. B*, **22**(9):3409–3420, 2017, `https://doi.org/10.3934/dcdsb.2017172`.

26. P.J. Pal, P.K. Mandal, Bifurcation analysis of a modified Leslie–Gower predator–prey model with Beddington–DeAngelis functional response and strong allee effect, *Math. Comput. Simul.*, **97**:123–146, 2014, `https://doi.org/10.1016/j.matcom.2013.08.007`.

27. H. Shen, C.H. Hsu, T.H. Yang, Fast–slow dynamics for intraguild predation models with evolutionary effects, *J. Dyn. Differ. Equations*, **32**:895–920, 2020, `https://doi.org/10.1007/s10884-019-09744-3`.

28. J.H. Shen, Canard limit cycles and global dynamics in a singularly perturbed predator–prey system with non-monotonic functional response, *Nonlinear Anal., Real World Appl.*, **31**:146–165, 2016, `https://doi.org/10.1016/j.nonrwa.2016.01.013`.

29. Y. Vera-Damin, C. Vidal, E. Gonzlez-Olivares, Dynamics and bifurcations of a modified Leslie–Gower-type model considering a Beddington–DeAngelis functional response, *Math. Methods Appl. Sci.*, **42**(9):3179–3210, 2019, `https://doi.org/10.1002/mma.5577`.

30. C. Wang, X. Zhang, Stability loss delay and smoothness of the return map in slow–fast systems, *SIAM J. Appl. Dyn. Syst.*, **17**(1):788–822, 2018, `https://doi.org/10.1137/17M1130010`.

31. C. Wang, X. Zhang, Canards, heteroclinic and homoclinic orbits for a slow-fast predator-prey model of generalized Holling type III, *J. Differ. Equations*, **267**(6):3397–3441, 2019, `https://doi.org/10.1016/j.jde.2019.04.008`.

32. C. Wang, X. Zhang, Relaxation oscillations in a slow–fast modified Leslie–Gower model, *Appl. Math. Lett.*, **87**:147–153, 2019, `https://doi.org/10.1016/j.aml.2018.07.029`.

33. R. Yafia, M.A. Aziz-Alaoui, Existence of periodic travelling waves solutions in predator prey model with diffusion, *Appl. Math. Model.*, **37**(6):3635–3644, 2013, `https://doi.org/10.1016/j.apm.2012.08.003`.